

Dear reviewers,

First of all, we would like to thank you for the constructive and detailed comments on our manuscript.

We have addressed the comments and suggestions provided. We have included the proposed modifications and clarifications in a new manuscript. It took us some time to address the changes due to the large number of participants and numerical models involved in the project.

Below you can find answers to the most important comments provided in the review:

1. Regarding the GDW approach and the comment: *Traditionally, apparent mass in aerodynamics is the unsteady part of the pressure loads and it is not connected to hysteresis due to time varying wake induction (which is what GDW does). I would describe GDW as a semi-analytical frozen wake variant of a vortex wake model.*

We have changed GDW description to: *In GDW, dynamic inflow is explicitly calculated by representing the induced velocity in terms of series expansion of radial and azimuthal basis functions within a governing equation that takes into account an apparent mass.*

A similar description and terminology can be found in the next references:

Peters, David A., and Cheng Jian He. "Correlation of measured induced velocities with a finite-state wake model." *Journal of the American Helicopter Society* 36, no. 3 (1991): 59-70.

Moriarty, Patrick J., and A. Craig Hansen. *AeroDyn theory manual*. No. NREL/TP-500-36881. National Renewable Energy Lab., Golden, CO (US), 2005. <https://doi.org/10.2172/15014831>

We have also slightly changed the FVW description to try to make more obvious the differences with regarding to the GDW:

*Dynamic inflow is intrinsically captured by FVW because induction is calculated directly from the time-dependent trailing and shed vorticity.*

2. Regarding the comment about FVW models: *FVW models are further categorized to lifting line, lifting surface and 3D panel. Not all of them use pre-calculated polars and this is an important distinction that should be incorporated in table 3.*

We agree on this and it is important to clarify this point. Accordingly, we have rearranged the models description (see lines 152-166 in the new manuscript):

*The participants used modeling approaches of different fidelity to study the system: blade element momentum (BEM) theory, dynamic BEM (DBEM) that accounts for dynamic inflow effect, generalized dynamic wake (GDW), free-vortex wake (FVW), and blade-resolved or actuator-line-based computational fluid dynamics (CFD).*

*The BEM, DBEM, GDW, some FVW and the actuator-line-based CFD approaches are based on the lifting line theory. In these approaches, the airfoil polar data is used as an input for the model. The airfoil polar provides information about the lift and drag coefficients as a function of the angle of attack. Participants can use the airfoil polar information as a look-up table (static polars approach) or account for unsteady airfoil aerodynamics. The unsteady airfoil aerodynamics accounts for the flow hysteresis in the lift and drag coefficients under unsteady wind and wind turbine operating conditions (e.g., blade pitch actuations). The flow hysteresis can occur during attached flow (e.g., linear region in the airfoil polar) or flow separation, including dynamic stall (e.g., nonlinear region in the airfoil polar). These unsteady effects are computed by the modeling tools and depend on the underlying theory considered. The lifting surface and 3D panel FVW as well as the blade-resolved CFD do not use the airfoil polar data as input. Instead, they use a surface mesh based on the blade geometry. One computer aided design (CAD) file of the blade was provided to the participants. In this case, it may be challenging to reproduce the airfoil polars behavior due to the relatively small Reynolds numbers during the experiment (mainly below 1E5). Small Reynolds numbers may increase the boundary layer thickness, resulting in larger drag and smaller lift coefficients.*

We also included a sentence to clarify that the models used by FVW participants in this project are based on the lifting line theory (line 190): *All FVW models used by participants are based on the lifting line theory.*

3. Comment about the low pass filtering: *In asymmetric flow conditions, 2P, 4P etc. harmonics appear in the loads of the blade rotating frame (system attached to the rotating blade) which become 3P, 6P etc. when transferred to the tower frame. These are not only due to tower shadow. So, by low pass filtering you may omit part of the aerodynamic unsteady response. A band stop filter would be preferable in this case. Unless you are sure that loads are described by a pure 1P response which*

*I doubt in the case of CFD or FVM. Or of course, if you are only interested in resolving the dynamic inflow effects due to the low frequency platform motion. In this case a proper explanation is required though.*

We are certain that the experiment included a rotor mass imbalance and probably an aerodynamic rotor imbalance due to the presence of 2P in the non-rotating reference system (tower). Since we were interested in the unsteady aerodynamic effects as a consequence of the platform motion (low frequency), we disregarded the information at 1P and above. Moreover, participants do not include any rotor asymmetry in their models. We agree that 3P is not only due to tower shadow. We make the comment about the 3P in the manuscript for readers to know that the expected tower shadow response won't be included in the outputs.

- Hot-wire measurements in the along-wind direction: *I would recommend the authors to remove the FVM results for the wake inflection point from figure 9. The answer why these results are pointless can be found in the explanation by the authors. It is also necessary to provide more information on how much is the ambient turbulence in the wind tunnel test data and how this is simulated by the CFD tools.*

We agree that FVM models have limitations predicting the wake behavior. We have modified the explanation and figure as follows:

Figure 7 (left) shows the corresponding longitudinal wind speed ( $u$ ) measured by the hot-wire probe and the output from the FVM and CFD participants. The wind speed in the figure corresponds to the average value at the location of interest during one rotor revolution. The CFD solutions are denoted with a solid line while the FVM solutions (12 outputs) are denoted by a gray area due to some limitations. For example, the wind speed obtained within the wake is a function of the wake length chosen by the FVM participants. Moreover, the lack of viscous diffusion in the FVM models makes the characterization of the wake recovery challenging in the absence of meandering from turbulence. Despite these limitations, we would expect a decent agreement between FVM approaches in the near wake region because, in this region, the viscous diffusion should not be driving the wake response. However, a significant spread of results was observed for FVM participants. Figure 7 (right) shows the inflection wake recovery point for the experiment and the CFD participants. This is the point where the wake velocity shows a minimum and from that point starts to recover. The outputs from individual FVM participants are not included for the reasons explained previously. It is also worth noting that the ambient turbulence observed in the wind tunnel should result in a shorter inflection wake recovery point. The ambient turbulence intensity during the testing was close to 2 % while participants considered a steady wind condition. The maximum wake velocity deficit observed in the experiment is around  $u/U_0 = 0.44$ . Most numerical models show a wind speed deficit like in the experiment. However, there are some differences regarding the inflection wake recovery point. For most CFD participants, the inflection wake recovery point occurs at a distance equal to or after 5.48 m (i.e., 2.3 diameters downwind).

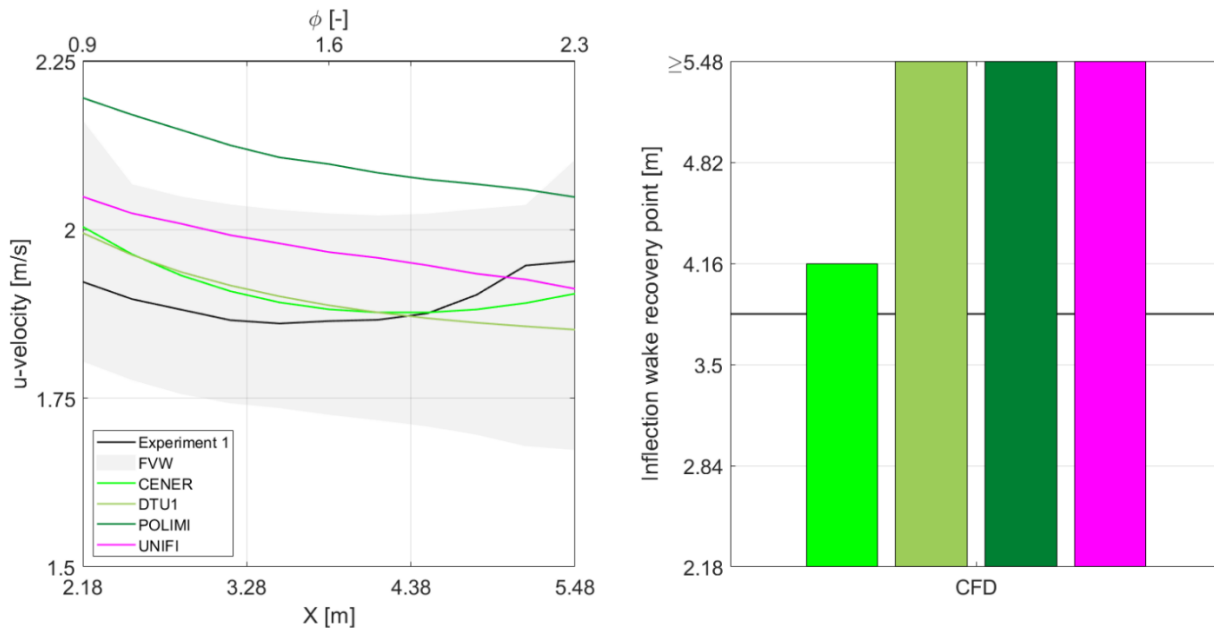


Figure 1: Left: Averaged hot-wire longitudinal velocity for one rotor revolution in the along-wind direction ( $y = 0.9$  m,  $z =$  hub height) during steady wind conditions. Right: Inflection wake recovery point location.

- Authors reviewed the manuscript to address any syntax and grammar errors.

Some additional comments based on the feedback provided in the accompanying pdf can be found below:

- a. We agree that the number of decimal positions in the blade description is beyond physical precision. We included this level of decimal positions to be consistent with previous work within the UNAFLOW project. For reference, previous studies considered 39 radial stations while in this project we simplified the definition to 20 radial stations. We wanted to provide the exact information that we were using so other researchers in the future can replicate it and use the results for verification and validation purposes.
- b. Additional information about what CFD participants included the wind tunnel walls and the hub nose and nacelle geometry has been included in the manuscript.
- c. Figure 2 has been modified to illustrate the two coordinate systems used in the project (i.e., where loads were measured and where they are compared).

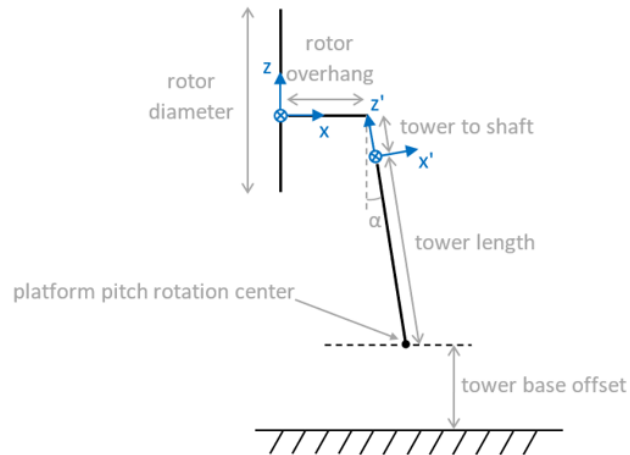
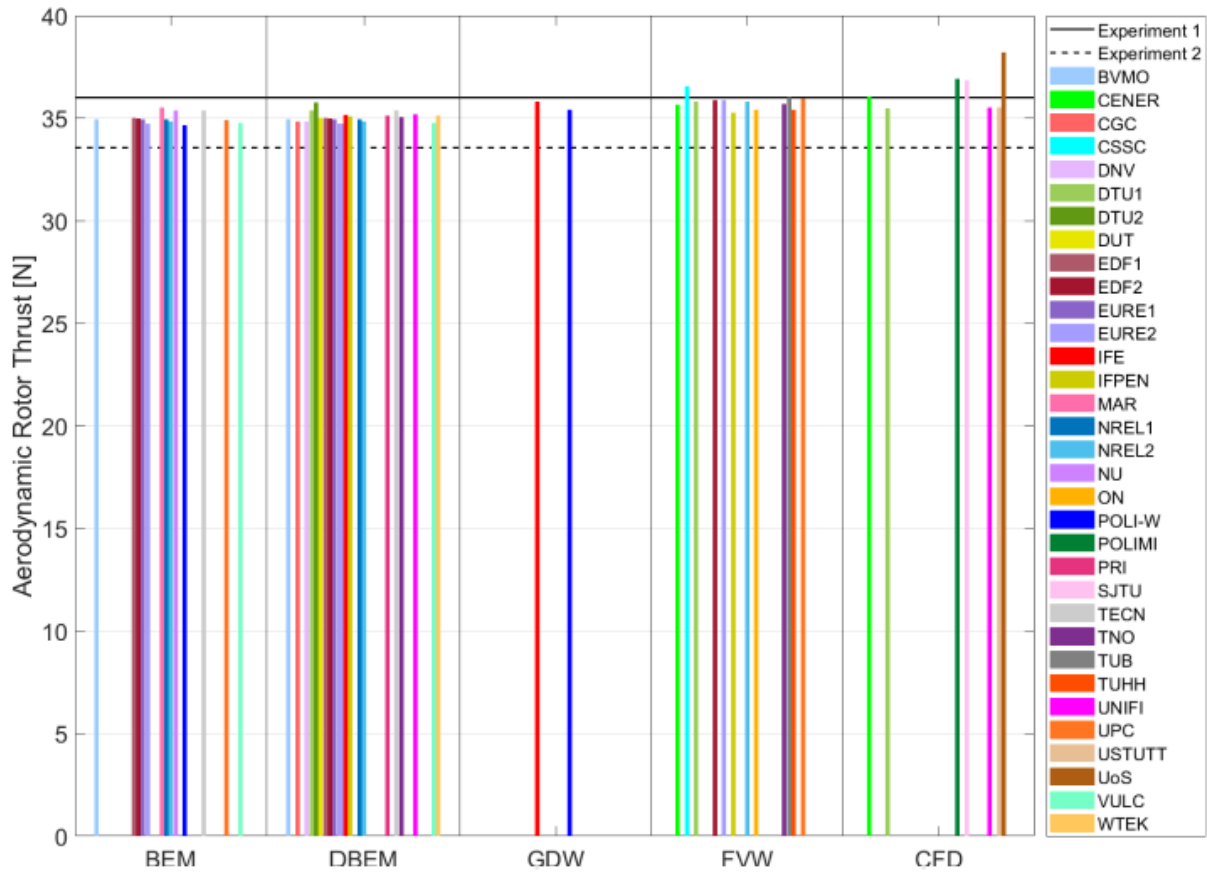


Figure 2: Schematic representation of the wind turbine system and the coordinate systems (hub fix and tower top).

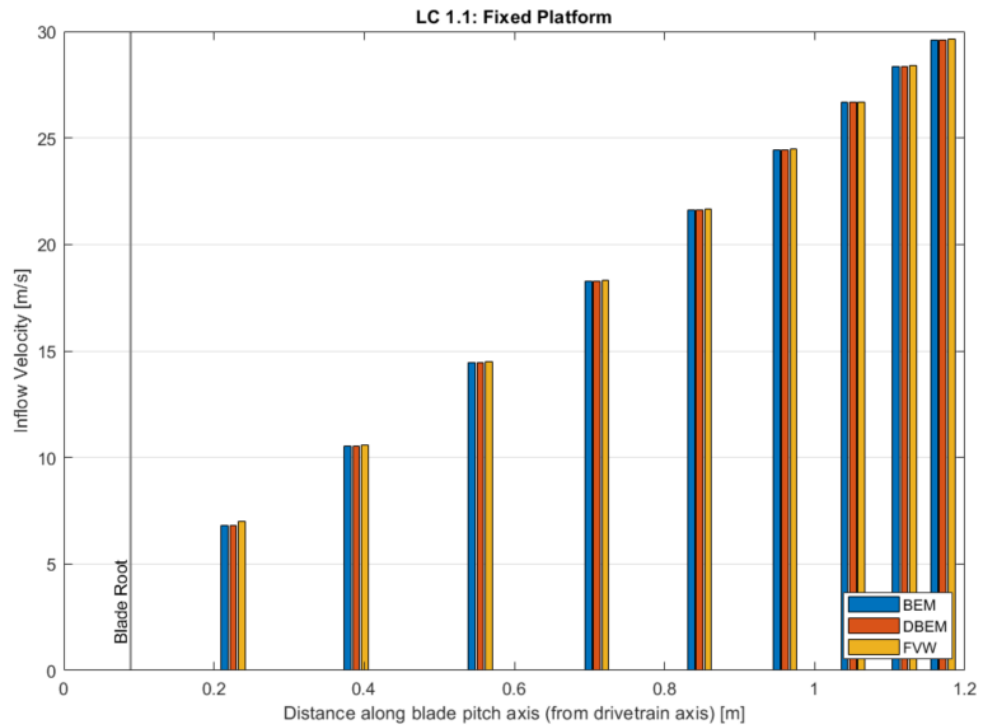
- d. Comment about thrust load in FVW being higher than BEM/DBEM: *Very illustrative that you have grouped the models according to the level of fidelity. It looks like FVW models tend to predict higher thrust than the BEM based models, although they use the same polars. Is there any explanation of this difference? I would guess that a reason could be the low Reynolds number of the test campaign. The inviscid nature of the wake generation process in these models does not comply with the low Reynolds conditions of the experiment?*



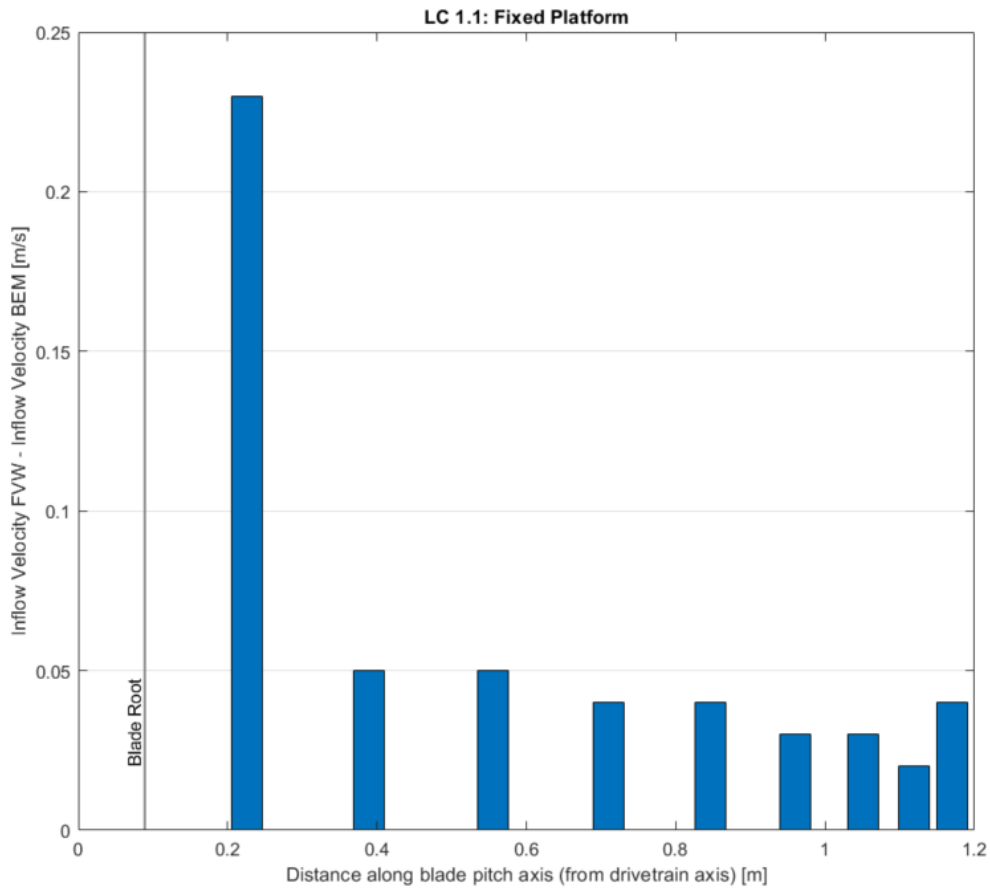
**Figure 3: Aerodynamic rotor thrust in steady wind conditions (load case 1.1)**

Your explanation could indeed make sense, but we have observed this trend for other, larger wind turbines, at higher Reynolds number. It appears that lifting-line FVW methods tend to return lower induced axial velocities than BEM, resulting in higher loads.

The below figure shows the local inflow velocity along the blade for the LC 1.1 (fixed platform condition). In this case we are using the same simulation tool (OpenFAST) and comparing different modeling approaches (e.g., BEM, DBEM and FVW).



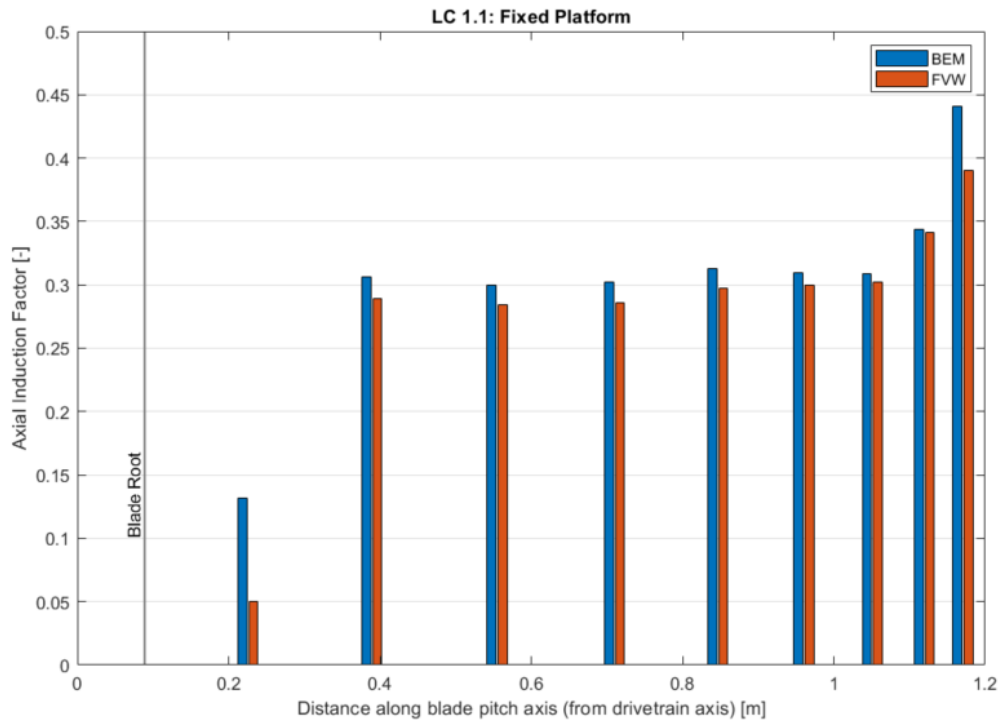
As expected, BEM and DBEM approaches return the same inflow velocity. For the FVW, the inflow velocity is slightly higher than for the BEM solution. This can be observed in the below figure, where we highlight the differences between FVW and BEM inflow velocities along the blade.



Similar behavior has been observed for other participants using FVW and BEM/DBEM solutions.

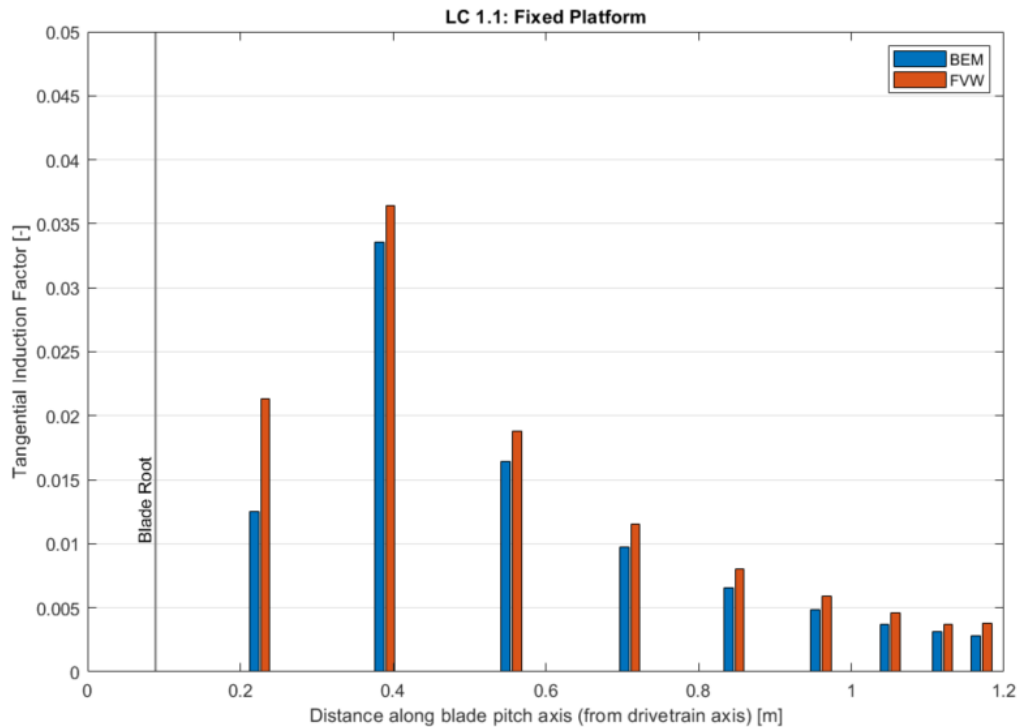
Since the rotor speed is fixed (240 rpm) and the incoming wind is the same (4.19 m/s), any differences in the local inflow velocity must come from the induction.

By comparing BEM and FVW in terms of axial induction factor along the blade, we obtained:



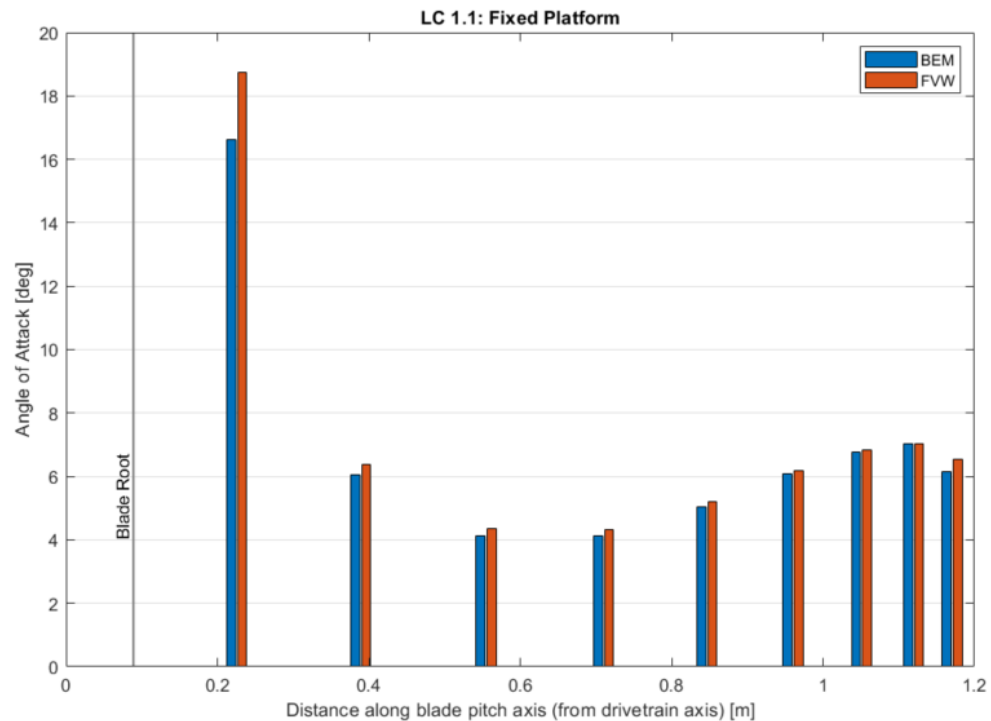
As can be observed, the axial induction factor ( $a$ ) of the FVW is always lower compared to the BEM. This implies that the longitudinal velocity in the FVW is higher.  $V_x = V_\infty * (1 - a)$

By comparing the tangential induction factor, we obtained:



As can be observed, the tangential induction factor ( $a'$ ) of the FVW is always higher compared to the BEM. This implies that the tangential velocity due to the rotor rotation in the FVW is higher. Although the variations here are small.  $V_y = \Omega * r * (1 + a')$

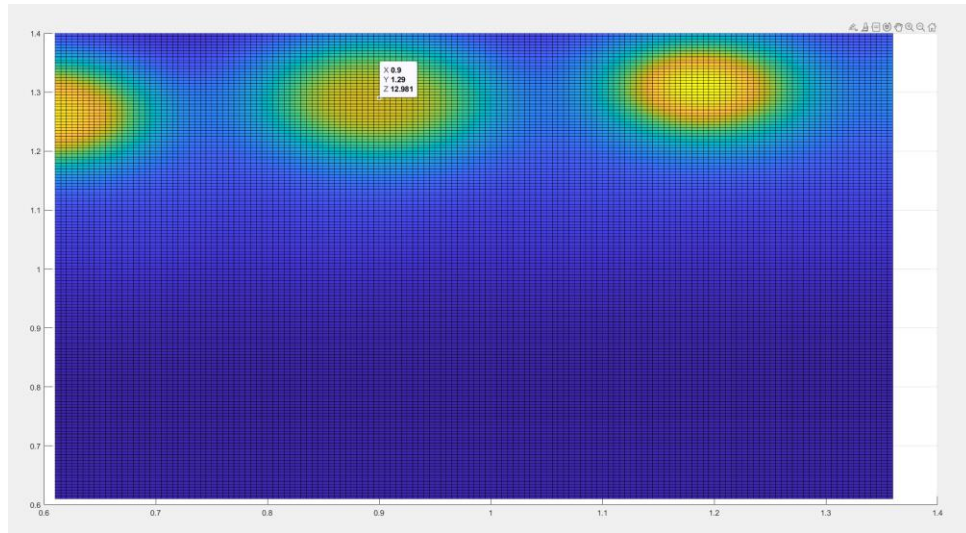
By comparing the angle of attack, we obtained:



As can be observed, the angle of attack of the FVW is always higher compared to the BEM. This is consistent since the changes in the axial induction factors are significant. The FVW clearly has larger longitudinal wind speeds due to the lower axial induction factors along the blade that translates into higher angles of attack.

Accordingly, we have included an explanation in the new manuscript as follows: *As Fig. 3 shows, most numerical models predict an aerodynamic thrust force that is within the values observed in the experiments. Only some FVW and CFD solutions are slightly above the values observed in Experiment 1. FVW solutions (based on the lifting line theory) return higher thrust values than BEM and DBEM solutions despite using the same airfoil polar data. When looking at the local inflow velocity along the blade (not shown), it can be noticed that the FVW models have slightly higher values. Since the rotational speed is fixed and the incoming wind is the same, this indicates that the FVW models have slightly different induction factors. By looking at the axial and tangential induction (not shown), FVW models have lower axial and higher tangential induction factors with both contributions adding to a higher local inflow velocity. Moreover, the lower axial induction factor in the FVW results in a higher angle of attack. Both, the higher local inflow velocity and the higher angle of attack, result in higher loads.*

- e. We have included a new reference to explain the statement about planar rotor. From the steady wind section: *No differences between static polars and unsteady airfoil aerodynamics are expected because the angle of attack at each blade radial station is constant, and the rotor is planar (Li et al., 2022).*  
Li, A., Gaunaa, M., Pirrung, G. R., Meyer Forsting, A., and Horcas, S. G.: How should the lift and drag forces be calculated from 2-D airfoil data for dihedral or coned wind turbine blades?, *Wind Energ. Sci.*, 7, 1341–1365, <https://doi.org/10.5194/wes-7-1341-2022>, 2022.
- f. PIV data: Why is TUB (FVW) vortex trajectory aligned with the CFD models and not the FVW models?  
We had some problems in the post-processing used to identify the vortex center trajectories for TUB. We looked more in detail at the output from this participant and recomputed the vortex center trajectory.



We could see that the vortex center was in reality aligned with other FWV participants. We have updated Figure 10 accordingly:

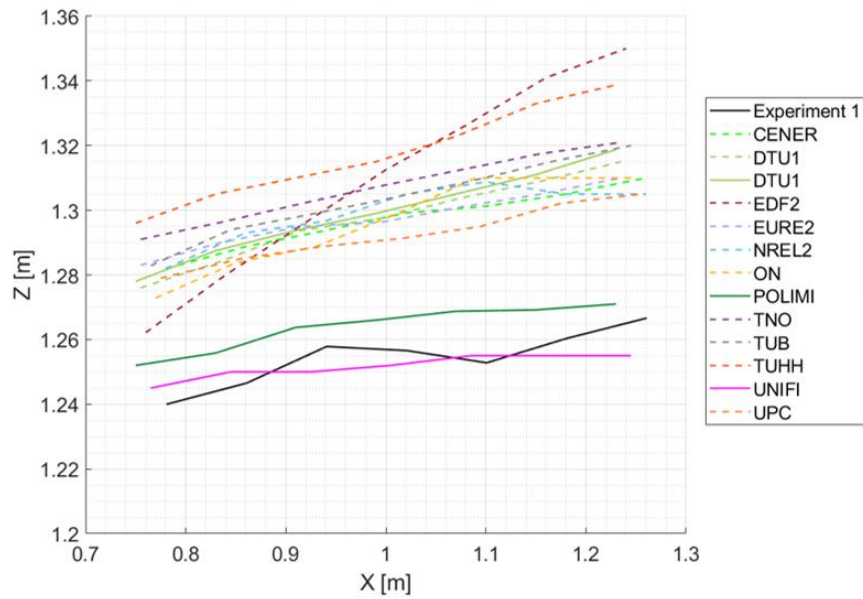


Figure 10: Averaged blade tip vortex trajectory in the PIV plane during steady wind.

All these changes have been addressed in the new manuscript.